Pierre-Emmanuel Mazeran[a], Moez Beyaoui[b], Maxence Bigerelle[a], Michèle Guigon[a]
[a]Laboratoire Roberval, UMR CNRS-UTC 6253, Université de Technologie de Compiègne, Compiègne, France
[b]Unité de Dynamique des Systèmes Mécaniques, Ecole Nationale d'Ingénieurs de Sfax, Tunisie

Determination of mechanical properties by nanoindentation in the case of viscous materials

A mechanical model based on a generalized Kelvin–Voigt model has been developed to explain and fit the nanoindentation curves realized on three amorphous polymers (PC, PMMA and PS). This model includes the responses of quadratic elastic (spring), viscoelastic (two Kelvin–Voigt elements), plastic (slider) and viscoplastic components (dashpot). It is able to fit nanoindentation curves during loading, unloading and hold time periods. With the values of the model parameters and the value of the contact area calculated with the Oliver and Pharr method, it is possible to calculate the values of the mechanical properties of the polymers. A good agreement is found between these values and those obtained with conventional methods.

Keywords: Nanoindentation; Polymer; Elastic modulus; Hardness; Viscosity

1. Introduction

The determination of the mechanical properties of bulk materials or thin films by instrumented indentation at a nanometer scale was developed and has been widely used during the last two decades [1, 2]. This technique is now currently used to determine the hardness, the elastic modulus or other mechanical properties on sufficiently low volumes to obtain a local measurement of the mechanical properties. Methods that allow determining the hardness H and the elastic modulus E by taking into account the elastic return of material during the unloading stage have been developed [3–5]. In the case of isotropic elastoplastic materials, the elastic modulus and the hardness can be given with excellent precision [3]. Nevertheless, in the case of materials whose mechanical response is time-dependent, such as polymers or biological materials, the description of the mechanical behavior by these two mechanical properties is obviously inadequate [6–19].

The development of the continuous stiffness measurement (CSM) method allows the continuous measurement of three parameters (load, contact stiffness and phase), then the calculation of the storage and loss moduli as well as the hardness of the material. It is an interesting opportunity but it remains limited to models with three parameters which are generally insufficient to describe the mechanical behavior of a material whose behavior depends on time [10, 14, 16, 18–21]. Another approach consists in fitting load–displacement curves using various mechanical models including viscous behavior [8, 10, 14, 16–17]. These models are based on the combination of elastic, viscoelastic, plastic and viscoplastic behaviors, modeled by springs, Kelvin–Voigt elements (spring in parallel to a dashpot), sliders and dashpots respectively [22].

These models allow fitting of experimental curves and determination of some mechanical properties with more or less convincing results in the quality of the fits and of the mechanical values that have been computed. In this work, an elastic viscoelastic plastic viscoplastic model (EVEPVP) (Fig. 1) is proposed to fit the indentation curves and to determine the mechanical properties of the indented materials. Each element of the model has an independent quadratic response: The root square of the load is proportional to the indentation depth and/or the indentation depth rate (Table 1). This model makes it possible to suitably adjust the displacement curves during the loading and unloading stage, as well as the hold load periods, after the loading and the unloading stages on three massive amorphous polymers: polycarbonate (PC), polymethyl methacrylate (PMMA) and polystyrene (PS). From the estimate of the contact area, it is possible to determine the relation between the displacements of each element and to go back to the material mechanical properties. Moreover, it shows that the values of the mechanical properties determined by our method are in good agreement with the quasi static values determined by the Oliver and Pharr method [5] and the values obtained from tensile tests.

2. Materials

Three amorphous polymers (PC, PMMA, PS) were tested. The amorphous polymers were preferred to semi-crystalline polymers to prevent any heterogeneity of crystallinity and thus of the mechanical properties.

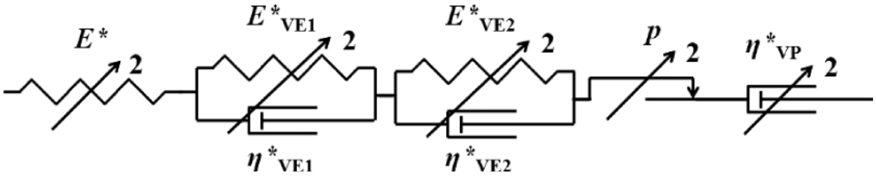

Fig. 1. Kelvin–Voigt generalized model with quadratic elements. The model is composed of a spring (elasticity), two Kelvin–Voigt elements (viscoelasticities), a slider (plasticity) and a dashpot (viscoplasticity).

Table 1. Relation between load and displacement and determination of the mechanical properties from the model parameters. k, n and p are the elastic, viscous and plastic parameters respectively that connect displacement or displacement rate to load. d, E, η and H are the displacement, the elastic modulus, the viscosity and the hardness respectively.

Behavior	Model	Mechanical law	Calculus of the mechanical properties
Elastic (E)	$\sqrt{F} = k_E\ d_E$	$S = 2\ E^* \sqrt{\frac{A}{\pi}}$	$E^* = k_E^2\ d_E \sqrt{\frac{\pi}{A}}$
Plastic (P)	$\sqrt{F} = p\ d_P$	$F = H\ A$	$H = \frac{p^2\ d_P^2}{A}$
Viscoelastic (VE)	$S = 2\ \left(k_{VE}^2 + 2\ k_{VE}\ n_{VE}\ \dot{\varepsilon}\right)\ d_{VE}$	$S = 2\ \left(E_{VE}^* + \eta_{VE}^*\ \dot{\varepsilon}\right) \sqrt{\frac{A}{\pi}}$	$E_{VE}^* = k_{VE}^2\ d_{VE} \sqrt{\frac{\pi}{A}}$ $\eta_{VE}^* = 2\ k_{VE}\ n_{VE}\ d_{VE} \sqrt{\frac{\pi}{A}}$
Viscoplastic (VP)	$\sqrt{F} = n_{VP}\ \dot{d}_{VP}$	$F = A\ \eta_{VP}\ \dot{\varepsilon}$	$\eta_{VP} = \frac{n_{VP}^2\ d_{VP}\ \ \dot{d}_{VP}}{A}$

The PC was provided by Axxis™ under the denomination Axxis™ PC and is ductile. The nominal mechanical properties (tensile modulus $E_{Tensile}$, yield strength R_e, tensile strength R_m and Poisson's ratio ν) are the following: $E_{Tensile} = 2.3$ GPa, $R_e = 60$ MPa and $\nu = 0.4$. The PMMA was provided by Altuglas™ under the denomination Altuglas™ Ex and is brittle. The nominal mechanical properties are $E_{Tensile} = 3.3$ GPa, $R_m = 74$ MPa, $\nu = 0.39$. The PS was provided by Goodfellow™ and is ductile. The nominal mechanical properties are $E_{Tensile} = 2.3–4.1$ GPa, $R_e = 30–100$ MPa, $\nu = 0.35$. Tensile tests were performed with the use of a Zwick™ Z010 tensile test machine at a strain rate of 0.011 s^{-1}. The elastic moduli obtained from the tensile tests were 2.24, 3.10 and 3.23 GPa for PC, PMMA and PS respectively.

3. Experimental protocol

All the indentation tests were carried out with a Nanoindenter XP from MTS™ using the continuous stiffness measurement (CSM) method with a frequency of 45 Hz and displacement amplitude of 2 nm. A Berkovich indenter was used. The indentation depth is calculated by including the defect tip (missing end of the tip compared to a perfect Berkovich geometry) using the method proposed by Hoeschetter et al. [6]. The calibration factor C that connects the contact area A to the contact depth h_c:

$$A = C\ h_c^2 \tag{1}$$

was calibrated using a fused silica sample ($C = 24.44$).

The contact depth h_c was calculated by using the Oliver and Pharr method [5]:

$$h_c = h_t - \varepsilon \frac{F}{S} \tag{2}$$

With h_t the indentation depth, F the load, S the contact stiffness and ε a geometrical coefficient equal to 0.75.

In order to make reliable use of the mechanical model and in particular the determination of the mechanical properties, it is therefore important to carry out indentation tests by using appropriate experimental protocols (sequence of load, unload and hold load periods) and parameters (load rate, hold load time).

3.1. Loading and unloading

The test is conducted at a constant loading rate/load ratio in order to obtain a constant strain rate during the loading stage, thanks to the application of the principle of geometrical similarity for pyramidal indenters [23]. For the unloading phase, it is extremely difficult to obtain a constant strain rate because the principle of geometrical similarity is not applicable due to the non-reversibility of the plastic deformation. Nevertheless, we put forth the hypotheses that an unloading process at a constant unloading rate/load ratio is

i) closest to the experimental conditions leading to a constant strain rate as compared to experiments at constant unloading rate
ii) that the strain rates obtained during the loading and unloading phase are equal if the loading rate/load and unloading rate/load are equal.

In addition, the strain rate must be sufficiently high to obtain a delayed response making it possible to describe the viscous behavior during the hold load plateaus and must be sufficiently low so that the material viscosity only moderately affects the indentation test and that the methods of analysis remain valid. The fact of using a constant unloading rate/load in our experimental conditions leads to a high initial unloading rate (typically of the mN · s^{-1}) at the beginning of the unloading, in good agreement with the specification imposed for viscous materials [9, 11–13].

3.2. Hold periods

Indentation curves in the case of the polymers often show an increase in the indenter depth (we will speak about secondary penetration) during the hold load plateaus after loading or the presence of the so called phenomenon of "nose" [6–9, 11] during the beginning of the unloading curve if the hold time is not sufficiently large. Thus, the Oliver and Pharr method is not perfectly adapted for viscous materials. Too short a hold load period before unloading, as compared to the unloading rate, leads to a too high measured slope of the unloading curve as compared to the slope that should be obtained for a pure elastic response. If the measured slope is too high, one obtains a too high elastic modulus. Thus, for polymers, the values of the elastic modulus measured by nanoindentation are generally higher than those measured by tensile test. It has been shown that the slope of the unloading curve should be recalculated to take into account the creep of the materials [9, 11–13]. For experiments conducted with a monotonic loading and hold depth period before unloading, Cheng et al. [12, 13] have proposed recomputing the correct elastic slope S from the experimental slope S_{Exp}. Ngan et al. [9, 11] proposed a similar correction formula for experiments conducted with a monotonic loading and hold load period before unloading, (which is the conventional case):

$$\frac{1}{S} = \frac{1}{S_{\mathrm{Exp}}} - \frac{\dot{h}_{h=h\max}}{\dot{F}_{h=h\max}} \tag{3}$$

Where $\dot{h}_{h=h\max}$ and $\dot{F}_{h=h\max}$ are the tip displacement rate just before unloading and the unloading rate respectively. This correction is valid for both viscoplastic [11] and viscoelastic materials [9]. This equation shows that the correction is not necessary if the displacement rate is low compared to the unloading rate. Thus, it explains why it is necessary to choose a long hold load period [7, 16, 19] and/or a high unloading rate [6]. Experimental results show on various samples that the values of hardness and elastic modulus become constant if the hold load period is more than a few minutes [6–7, 16, 19].

The presence of the "nose" is evidence that the mechanical behavior of the indented material depends on time. This phenomenon can be interpreted as a viscoelastic and/or viscoplastic phenomenon. To discriminate the kind of behavior, it is thus important to check that the phenomenon is reversible (viscoelastic) or irreversible (viscoplastic) at the observation scale of time, by imposing on the test a hold load plateau after unloading. Then, it should be made sure that the secondary penetration is almost completed before beginning the unloading phase to ensure that a continuation of the penetration during the hold load plateaus after unloading is not due to the continuation of a viscoelastic response to the loading phase. Thus, the tests should be carried out with a sufficiently large duration of the hold load plateau so that the material relaxation times can be highlighted. Figure 2 shows a viscoelastic return of the material during the hold load periods after unloading which makes it possible to confirm that the behavior is mainly viscoelastic.

According to these considerations, all the tests were carried out with the following procedure. The material was indented with a constant loading rate/load ratio equal to 0.03 s^{-1} until an indentation depth of 3 000 nm. The load was then maintained constant for a period of 600 s in order to be able to observe the secondary penetration. This value is generally high enough as polymers show relaxation times of a few minutes [8, 10, 14, 17]. The material was then unload at a constant unloading rate/load ratio (and equal at the loading rate/load) in order to obtain a quasi constant strain rate until a load value equal to 50 % of the maximum load was reached. After unloading, the load was maintained constant for a period of 600 s. These experimental conditions lead to a ratio $\dot{h}_{h=h\max}/\dot{F}_{h=h\max}$ that is typically two orders of magnitude lower than the inverse of S_{Exp}, thus the Oliver and Pharr method [5] could be used directly without the need of the correction equation proposed by Ngan et al. [11].

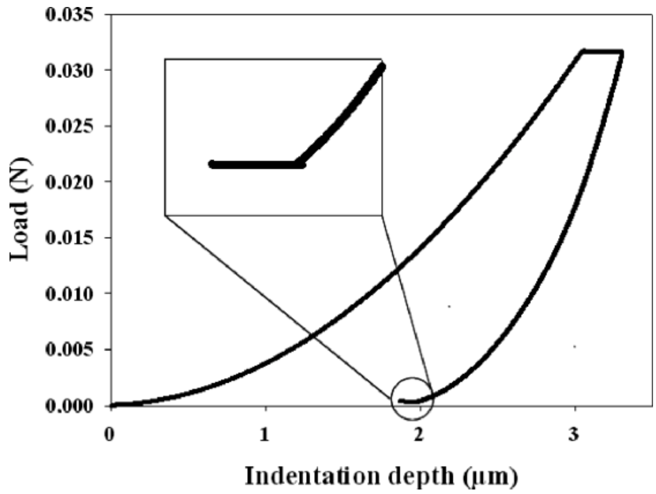

Fig. 2. Load as a function of the indentation depth in the case of a PMMA sample ($\dot{F}/F = 0.03\ s^{-1}$). One can see an increase and a decrease of the indentation depth during the hold load plateaus.

4. Modeling of the indentation test

4.1. Fitting the experimental curves with EVEPVP model

EVEPVP models are classically used to describe and fit time-dependent experiments conducted on polymers. They are based on a combination of a linear spring(s), dashpot(s) and slider(s) either in parallel or in series [22]. To further extend this model to nanoindentation experiments, this kind of model should be modified to give a quadratic response as nanoindentation experiments are generally conducted with pyramidal indenters leading to a quadratic dependence between load and displacement.

For perfectly rigid conical or pyramidal indenters on a elastic material, the relation between load and indentation depth is given by [24]:

$$F = \frac{2}{\pi} E^* h_t^2 \tag{4}$$

Where E^* is the reduced modulus. This equation is similar to the response of a quadratic spring:

$$\sqrt{F} = k_E d_E \tag{5}$$

Where k_E and d_E are the stiffness and the displacement of the quadratic spring respectively. Furthermore, if the indentation is purely elastic one can assume that the elastic response could be modeled by a quadratic spring taking $h_t = d_E$.

As well, according to the Oliver and Pharr model, the definition of hardness for conical or pyramidal indenters on a perfectly plastic material ($h_c = h_t$) gives:

$$F = H\,A = H\,C\,h_t^2 \qquad (6)$$

This equation is similar to the response of a quadratic slider:

$$\sqrt{F} = p\,d_P \qquad (7)$$

Where p is the parameter connecting the load and the displacement of the plastic element and d_P is the displacement of the plastic element. However, because plasticity is not reversible, d_p could not be less than $\sqrt{F_{Max}}/p$, where F_{Max} is the maximum load applied from the beginning of the test. For viscoplastic behavior, the relation could be described by a quadratic dashpot [8, 17]:

$$\sqrt{F} = n_{VP}\,\dot{d}_{VP} \qquad (8)$$

Where n_{VP} and d_{VP} are the viscosity and the displacement of the viscoplastic element. Furthermore, viscoelastic behavior like a quadratic Kelvin–Voigt element (spring and dashpot in parallel), leads to the following equation:

$$\sqrt{F} = k_{VE}\,d_{VE} + n_{VE}\,\dot{d}_{VE} \qquad (9)$$

Where k_{VE}, n_{VE} and d_{VE} are the stiffness, viscosity and displacement of the viscoelastic element respectively.

All these elements have a quadratic response: The root square of the load is proportional to the elementary indentation depth and/or the elementary indentation depth rate (Table 1). These equations are simple and could be easily used to compute the elementary displacement whatever the load–time history. Then it is possible to construct an analytical quadratic model with these quadratic elements in series to reproduce indentation curves taking:

$$h_t = d_E + d_{VE} + d_P + d_{VP} \qquad (10)$$

Schiffman [14] shows that a generalized Kelvin–Voigt model (n Kelvin–Voigt elements in series) is much better than a Burger model (a Maxwell and a Kelvin–Voigt element in series) to fit experimental curves. This means that the viscoelastic behavior could not be modeled by only one Kelvin–Voigt element. Furthermore, creep compliance tested by conventional tensile tests show that amorphous polymers with high molecular weight and narrow molecular distributions present two relaxation times [25]. Two relaxation times or more are also used to fit nanoindentation curves [10, 14].

Our EVEPVP model (Fig. 1) contains an elastic (spring), two viscoelastic (two Kelvin–Voigt elements), a plastic (slider), and a viscoplastic component (dashpot). In accordance with our operating conditions, two Kelvin–Voigt elements are sufficient to describe the viscoelastic behavior of the three indented polymers. The use of one Kelvin–Voigt element leads to a poor quality fit of the experimental curves and the use of a third Kelvin–Voigt element is not necessary to fit the experimental curves very well. The fact that the model is based on two Kelvin–Voigt elements does not means that the material has only two relaxation times. A short relaxation time (much less than the (un)loading stage time) cannot be distinguished from the elastic behavior and a long relaxation time (much more than the hold load time) cannot be distinguished from viscoplastic behavior. Thus, it is uncertain if the mechanical behavior fitted by the viscoplastic element is viscoplastic or viscoelastic behavior with a very long relaxation time. It has already been shown that polymers present very long recovery times after unloading [26, 27] and the authors have notice that the residual imprints on PMMA samples disappear with time.

The fitting of the experimental curve is realized by the following procedure: First of all, the load as a function of time is extracted from experimental data and converts into analytical load–time equations for the load, unload and hold load periods in order to be

i) able to compute the displacements of all the elements as a function of time
ii) check that the analytical load–time equations reproduce perfectly the experimental curve.

Then, the elementary displacements are computed and summed to obtain the indentation depth as a function of time. This curve is then compared to the experimental one and the difference between the two curves is computed by the integration of the gap between them. The difference between the two curves is then minimized by adjusting manually the model parameters one by one. For each material, three experimental curves are fitted: The difference between the values of the same model parameters computed from two different curves is generally less than 5 % except for the viscoplastic element for which the difference could be larger than 50 %. This difference is explained by the fact that the indentation test is conducted over too long a time (typically half an hour) to prevent any drift. Then, the viscoplastic element fits both the drift and the viscoplastic behavior of the material. Nevertheless, the displacement of the viscoplastic element is small as compared to the other ones, and we can conclude that the materials have very little viscoplastic behavior as compared to their viscoelastic behavior. Nevertheless, the fitting of the experimental curves by this model is very satisfactory as observed in Fig. 3. Indeed, one can see for the three indented polymers that the experimental curves are very well fitted even for partial unloading going up to 50 % of the maximum loading. This shows that this easy-to-use model could be used with confidence.

4.2. Model limitations

When a quadratic elastic–plastic model is used, one would obtain a quadratic unloading curve. This would not allow reproducing the experiments of unloading curves observed for elastoplastic material: Indeed, Oliver and Pharr showed that the experimental unloading curves for elastoplastic materials can be adjusted by a power law for which the exponent is close to 1.5. This value corresponds to the unloading curve of a perfectly elastic material indented by a parabolic indenter [5]. Later, Bolshakov and Pharr [28] confirmed by numerical simulation that the unloading curves for elastoplastic material should have an exponent power close to 1.5. This phenomenon is due to the fact that the pressure distribution is similar in an elastoplatic material indented by a pyramid and in an elastic material indented by a parabolic indenter. It has been shown that the unloading curves in the case of a viscoelastic material can be fitted by a power law whose exponent is much more than 1.5 [19] which means that the exponent of the unloading curve is also governed by the viscoelastic behavior of the material or that the pressure distribution is probably not similar to those found for elastoplastic-material. Nevertheless, by using the EVEPVP model, it is perfectly possible to reproduce the general shape of the unloading curves of a viscoelastic material because they present exponents that can be much higher than 1.5 and close to those observed experimentally.

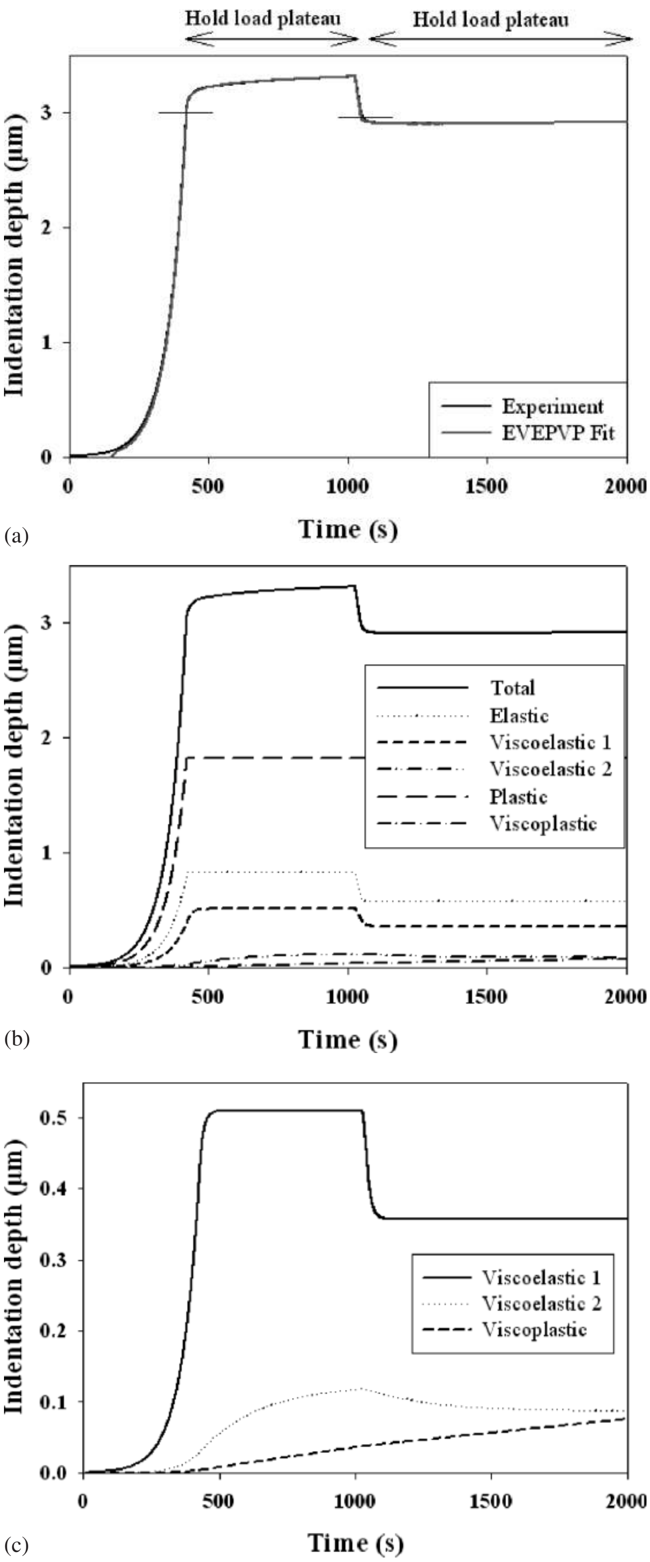

Fig. 3. Indentation depth as a function of time in the case of the indentation of a PC sample ($\dot{F}/F = 0.03\ s^{-1}$). (a) An excellent agreement is found between the experimental curve and the EVEPVP model fit. The horizontal lines mark the beginning of the hold load plateaus. (b) The total displacement of the model is the sum of the elementary displacements of the model components. (c) Zoom on the viscous elementary displacements of the model.

To validate the model it would be interesting to practice several strain rates to check that the model parameters are quite constant whatever the strain rate. Unfortunately, the applicable strain rates making it possible to obtain reproducible indentation curves do not cover an important domain. Indeed, for strain rates higher than 0.1 s^{-1}, the curves are generally not very reproducible and are strongly disturbed. With low strain rates (lower than 0.01 s^{-1}), the drift of the apparatus becomes almost equal to the indentation rate in particular during the hold load plateaus. Thus, it is very hard to obtain reproducible curves using a low strain rate. In these conditions, applicable strain rates cover less than one decade.

Obviously, the proposed mechanical model does not make it possible to adjust in a perfect way all indentation curves. Furthermore, the same curve can be adjusted by several sets of parameters with slightly different parameter values leading to approximately the same fit quality. It is thus difficult to know if a set of parameters or another one is most appropriate. It would be necessary to reproduce the indentation tests by varying the operating conditions and in particular the strain rates on great intervals to fix the problem but it is not possible to conduct them in the actual condition.

In addition, the stresses applied during an indentation test are triaxial. During the loading stage at a constant loading rate/load ratio, the principle of geometrical similarity makes it possible to say that the stress field is geometrically equivalent whatever the indentation depth and that the contact radius is proportional to the indentation depth. As a consequence we can affirm that a quadratic EVEPVP model is valid during the loading phase but probably not valid for the unloading phase.

During hold load plateaus, the penetration increases or decreases. The stress field is modified. Nevertheless it is noted in our experiments that the contact stiffness remains roughly proportional to the indentation depth during the hold load plateaus after loading and during the unloading stage until a load equal to about 25 % of the maximum load value is reached (Fig. 4). This allows us to make the hypothesis, thanks to Sneddon's equation, that the contact area is proportional to the square of the indentation depth and that a quadratic model remains relevant for most of the unloading stage.

4.3. Comparison with other methods

The EVEPVP model presented in this article could be considered as a synthesis of the models and methods proposed in the literature. Our approach is close to the method proposed by Oyen and Cook [8, 17]. Their model is adapted to their experiments that do not include a hold load plateau after unloading. This model does not include Kelvin–Voigt elements and will then fail to fit the viscoelastic return during hold load plateaus after unloading. Liu et al. [16] and Dub and Trunov [18] used a Burger model with just one Kelvin–Voigt element. Schiffmann [14] proposed both a Burger model and a generalized Kelvin–Voigt model. Yang et al. [10] used an EVEPVP model but failed to compute all the mechanical properties of the material.

5. Calculation of the mechanical properties

The parameters of the mechanical model allow connecting the load to displacements of the various elements. These parameters make it possible to fit the experimental curves

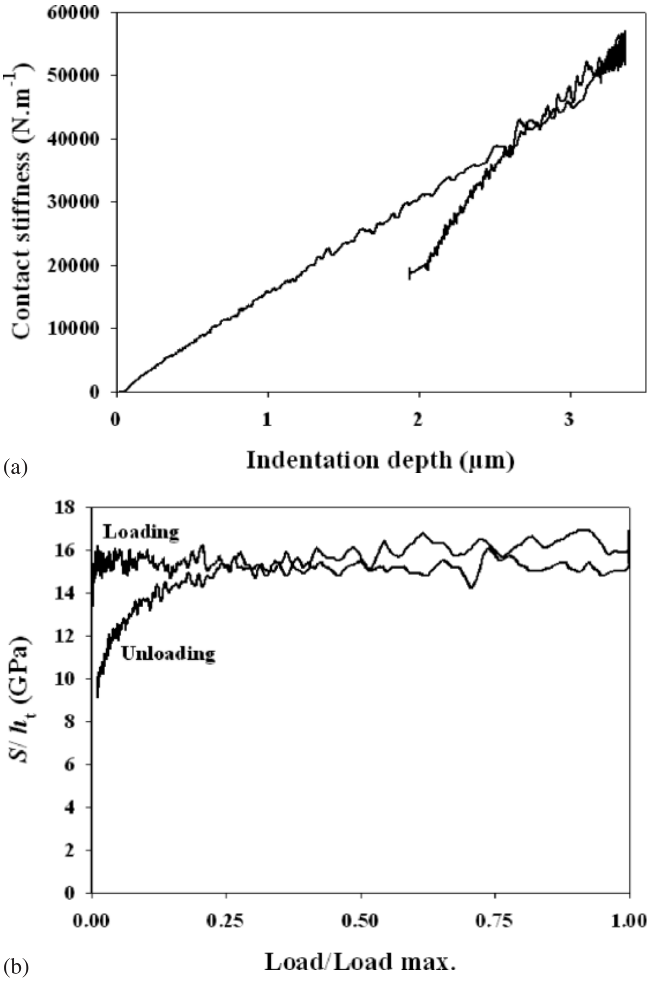

Fig. 4. (a) Contact stiffness as a function of the indentation depth for a PC sample ($\dot{F}/F = 0.03\ \mathrm{s}^{-1}$). (b) Ratio of the contact stiffness to indentation depth as a function of the relative load. One can see that the contact stiffness is proportional to the indentation depth since the unloading load is more than 25 % of the maximum load.

very satisfactorily, which makes us trustful on the relevance of the model. Nevertheless, they are of limited interest if it is not possible to calculate the mechanical properties of indented materials. To make the transition between the model parameters and the mechanical properties, it is necessary to connect the usual mechanics laws to the model equations.

Equation (5) models the elastic element. If this equation is squared and differentiated, the stiffness is given by:

$$S = \frac{\dot{F}}{\dot{d}_\mathrm{E}} = 2\ k_\mathrm{E}^2\ d_\mathrm{E} \tag{11}$$

With identification with the Sneddon equation [24],

$$S = 2\ E^*\ \sqrt{\frac{A}{\pi}} \tag{12}$$

It follows that:

$$E^* = k_\mathrm{E}^2\ d_\mathrm{E}\sqrt{\frac{\pi}{A}} \tag{13}$$

Equation (9) models the viscoelastic element. The strain rate is defined by:

$$\dot{\varepsilon} = \frac{\dot{d}_\mathrm{VE}}{d_\mathrm{VE}} \tag{14}$$

So Eq. (9) becomes:

$$\sqrt{F} = (k_\mathrm{VE} + n_\mathrm{VE}\ \dot{\varepsilon})\ d_\mathrm{VE} \tag{15}$$

If this equation is squared and differentiated and the strain rate is maintained constant, the stiffness is given by:

$$\begin{aligned} S &= \frac{\dot{F}}{\dot{d}_\mathrm{VE}} = 2\ (k_\mathrm{VE} + n_\mathrm{VE}\ \dot{\varepsilon})^2\ d_\mathrm{VE} \\ &= 2\ \left(k_\mathrm{VE}^2 + 2\ k_\mathrm{VE}\ n_\mathrm{VE}\ \dot{\varepsilon} + n_\mathrm{VE}^2\ \dot{\varepsilon}^2\right)\ d_\mathrm{VE} \end{aligned} \tag{16}$$

If the strain rate is small as compared to the other terms of the equation, it becomes:

$$S = 2\ \left(k_\mathrm{VE}^2 + 2\ k_\mathrm{VE}\ n_\mathrm{VE}\ \dot{\varepsilon}\right)\ d_\mathrm{VE} \tag{17}$$

Sneddon's equation is extended to the viscoelastic behavior by admitting that the contact stiffness is proportional to the contact radius multiplied by the sum of the elastic component E_VE^* and of the strain rate multiplied by the viscous component η_VE^* of the viscoelastic modulus:

$$S = 2\ \left(E_\mathrm{VE}^* + \eta_\mathrm{VE}^*\ \dot{\varepsilon}\right)\ \sqrt{\frac{A}{\pi}} \tag{18}$$

With identification with Eq. (17), one obtains:

$$E_\mathrm{VE}^* = k_\mathrm{VE}^2\ d_\mathrm{VE}\sqrt{\frac{\pi}{A}} \tag{19}$$

$$\eta_\mathrm{VE}^* = 2\ k_\mathrm{VE}\ n_\mathrm{VE}\ d_\mathrm{VE}\sqrt{\frac{\pi}{A}} \tag{20}$$

Equation (7) models the plastic element and the hardness is defined by:

$$H = \frac{F}{A} \tag{21}$$

Combining the two equations, it becomes

$$H = \frac{p^2\ d_\mathrm{P}^2}{A} \tag{22}$$

Lastly, Eq. (8) models the viscoplastic element. If we compare to viscoplastic behavior:

$$F = A\ \eta_\mathrm{VP}\ \dot{\varepsilon} \tag{23}$$

Where η_VP is the viscoplasticity. The strain rate is defined by:

$$\dot{\varepsilon} = \frac{\dot{d}_\mathrm{VP}}{d_\mathrm{VP}} \tag{24}$$

Leading to

$$\eta_\mathrm{VP} = \frac{n_\mathrm{VP}^2\ d_\mathrm{VP}\ \dot{d}_\mathrm{VP}}{A} \tag{25}$$

Because the model parameters and the displacements are known, it is thus possible to determine the values of the various mechanical properties of the model if the contact area is known (Table 1). At the beginning of the unloading, the contact area could be calculated from the Oliver and Pharr method. As pointed out previously, the Oliver and Pharr method could be used without any correction according to our operating conditions. Then, we are able to compute all the mechanical properties of our three polymers; this is one of the major points of interest of this method.

Table 2 presents the values resulting from this calculation and shows that the values resulting from the EVEPVP model are in conformity with less than 30 % of the values determined by tensile test ($\dot{\varepsilon} = 0.011\ s^{-1}$) and nanoindentation ($\dot{F}/F = 0.01\ s^{-1}$ and hold load period = 600 s) by using the Oliver and Pharr method: The equivalent reduced elastic modulus is the apparent elastic modulus computed with the generalized Kelvin–Voigt model using the mechanical properties calculated from the EVEPVP model and a strain rate equal to 0.01 s^{-1} according to the following equation:

$$\frac{1}{E^*_{\text{Equivalent}}} = \frac{1}{E^*_{\text{E}}} + \frac{1}{E^*_{\text{VE1}} + \dot{\varepsilon}\,\eta^*_{\text{VE1}}} + \frac{1}{E^*_{\text{VE2}} + \dot{\varepsilon}\,\eta^*_{\text{VE2}}} \tag{26}$$

Then, the equivalent elastic modulus is computed with the bulk nominal value of the Poisson's ratio:

$$E_{\text{Equivalent}} = E^*_{\text{Equivalent}}\left(1 - \nu^2\right) \tag{27}$$

The value of the equivalent modulus is then compared to the value of the elastic modulus obtained using the classical Oliver and Pharr method and tensile test. One can see that the values of the elastic moduli and hardnesses are in relative good agreement whatever the method. Thus, these values make the authors confident in the fact that the EVEPVP model is able to determine in a relatively reliable way the mechanical behavior under our experimental conditions and moreover the values of the viscous properties of the material, values that cannot be computed easily with nanoindentation experiments. It should be noted that the values of the viscoplastic component are high, which means that the viscoplastic behavior is very modest. Furthermore, it is not possible to be sure if this behavior is viscoelastic with a very long time relaxation time or viscoplastic. One can thus consider that the three polymers have essentially elastic, viscoelastic, plastic behavior and that the use of an elastic-plastic-viscoplastic model would be inadequate for these polymers. The elastic and viscoelastic components of the EVEPVP model are similar to a generalized Kelvin–Voigt model. They are used to compute the viscoelastic behavior of the material as a function of the frequency using the classical generalized Kelvin–Voigt model equations. Figure 5 presents the complex elastic modulus and the tan(δ) of the 3 indented polymers as a function of the frequency. One can see that the curve of tan(δ) as a function of the frequency is similar to tan(δ) versus temperature curves already published in the literature for amorphous and semi-crystalline PET [29]. Thus, the authors are confident in the fact that nanoindentation experiments are able to give frequency dependent elastic properties. The two relaxation times of the three materials are typically of half a minute and 10 min whatever the polymers (Table 2). Even if the relaxation times are dependent on the molecular weight, these values are in relative good agreements with values extracted from nanoindentation experiments [10, 14]. For example, in the case of the PC, the values of the two relaxation times computed in this study are 27 and 445 s, which are very close to the values found by Schiffman [14] (34 and 448 s).

In further work, values of the viscoelastic properties determined by our method will be compared with values obtained with classical dynamic mechanical analysis experiments for the same samples. It will help to refine and validate our approach. Furthermore, a generalized Kevin–Voigt model will be integrated in finite element simulation to check if it is possible by reverse approaches to fit experimental curves and compute the values of the mechanical properties of such polymers by this way.

6. Conclusion

We showed that a simple analytical mechanical model is able to fit very well the indentation curves carried out on

Table 2. Value of the mechanical properties calculated from the EVEPVP model, the Oliver & Pharr method and by tensile test. The equivalent elastic modulus is the apparent elastic modulus computed using the mechanical properties calculated from the EVEPVP model for an indentation test conducted at a loading rate/load equal to 0.01 s^{-1}.

Method	Mechanical behavior	Mechanical properties	Polymer		
			PC	PMMA	PS
Nanoindentation with EVEPVP model	Elastic	E^*_{E} (GPa)	4.84	9.98	9.48
	1st viscoelastic	E^*_{VE1} (GPa)	7.83	5.18	8.29
		η^*_{VE2} (GPa s)	214	213	178
		Relaxation time (s)	27	41	21
	2nd viscoelastic	E^*_{VE2} (GPa)	30.3	13	20.8
		η^*_{VE2} (GPa s)	13 500	9 940	8 450
		Relaxation time (s)	445	767	406
	Plastic	H_{p} (GPa)	0.16	0.186	0.235
	Viscoplastic	η_{VP} (GPa s)	108	124	156
	Reduced equivalent modulus	$E^*_{\text{Equivalent}}$ (GPa)	3.20	4.07	4.66
	Poisson's ratio	ν	0.4	0.39	0.35
	Equivalent modulus	$E_{\text{Equivalent}}$ (GPa)	2.68	3.45	4.10
Nanoindentation with Oliver & Pharr method	Elastic	E_{OP} (GPa)	2.22	3.34	3.90
	Plastic	H_{OP} (GPa)	0.157	0.192	0.186
Tensile test	Elastic	E_{Tensile} (GPa)	2.24	3.1	3.23

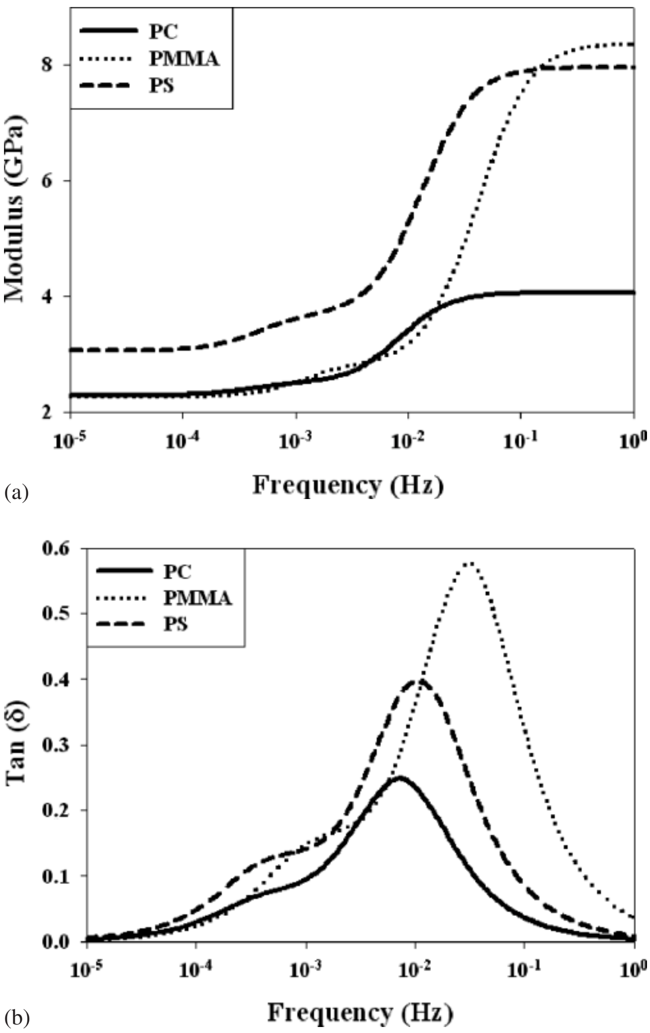

Fig. 5. (a) Complex modulus and (b) tan(δ) computed from the values of the elastic and the viscoelastic properties as a function of the frequency.

three amorphous polymers. This model is composed of independent, viscoleastic, plastic and viscoplastic elements whose response is proportional to the root square of the load. The data of the mechanical model could be converted into mechanical properties by establishing a relation between the specific displacement of each element and the contact area determined by the Oliver and Pharr method. One then observes a good agreement between the values determined by this method and the values resulting from the traditional Oliver and Pharr method and from the tensile test. It comes out from this analysis that the EVEPVP model and the method described in this article could be useful to establish the mechanical behavior and compute with a reasonable accuracy the values of the mechanical properties of viscous materials.

References

[1] W.C. Oliver, G.M. Pharr: J. Mater. Res. 19 (2004) 3. DOI:10.1557/jmr.2004.19.1.3
[2] A.C. Fischer-Cripps: Nanoindentation, Springer New-York (2002).
[3] M.F. Doener, W.D. Nix: J. Mater. Res. 1 (1986) 601. DOI:10.1557/JMR.1986.0601
[4] J.L. Loubet, J.M. Georges, O. Marchesini, G. Meille: J. Tribology 106 (1984) 43. DOI:10.1115/1.3260865
[5] W.C. Oliver, G.M. Pharr: J. Mater. Res. 7 (1992) 1564. DOI:10.1557/JMR.1992.1564
[6] G. Hochstetter, A. Jimenez, J.L. Loubet: Macromol. Sci. Phys. 38 (1999) 681. DOI:10.1080/00222349908248131
[7] T. Chudoba, F. Richter: Surf. Coat. Technol. 148 (2001) 191. DOI:10.1016/S0257-8972(01)01340-8
[8] M.L. Oyen, R.F. Cook: J. Mater. Res. 18 (2003) 139. DOI:10.1557/JMR.2003.0020
[9] B. Tang, A.H.W. Ngan: J. Mater. Res. 18 (2003) 1141. DOI:10.1557/JMR.2003.0156
[10] S. Yang, Y.W. Zhang, K. Zeng: J. Appl. Phys 95 (2004) 3655. DOI:10.1063/1.1651341
[11] A.H.W. Ngan, H.T. Wang, B. Tang, K.Y. Sze: Int. J. Solids Structures 42 (2005) 1831. DOI:10.1016/j.ijsolstr.2004.07.018
[12] Y.T. Cheng, C.M. Cheng: Mat. Sci. Eng. A 409 (2005) 93. DOI:10.1016/j.msea.2005.05.118
[13] Y.Y. Cheng, C.M. Cheng, W. Ni : Mat. Sci. Eng. A 423 (2006) 2. DOI:10.1016/j.msea.2005.09.134
[14] K.I. Schiffmann: Int. J. Mat. Res. 97 (2006) 9.
[15] M. Vanleene, P.E. Mazeran, M.C. Ho Ba Tho: J. Mat. Res. 21 (2006) 2093. DOI:10.1557/jmr.2006.0255
[16] C.K. Liu, S. Lee, L.P. Sung, T. Nguyen: J. Appl. Phys. 100 (2006) 033503 – 1 – 9.
[17] R.F. Cook, M.L. Oyen: Int. J. Mat. Res. 98 (2007) 5.
[18] S.N. Dub, M.L. Trunov: J. Phys. D: Appl. Phys. 41 (2008) 070424. DOI:10.1088/0022-3727/41/7/074024
[19] M. Beyaoui, P.E. Mazeran, M.F. Arvieu, M. Bigerelle, M. Guigon: Int. J. Mat. Res. 100 (2009) 7.
[20] N. Bruselle-Dupend, D. Lai, X. Feaugas, M. Guigon, M. Clavel: Polym. Eng. Sci. 43 (2003) 501. DOI:10.1002/pen.10041
[21] I. Yakimets, D. Lai, M. Guigon: Mech. Time-Depend. Mater. 11 (2007) 47. DOI:10.1007/s11043-007-9031-8
[22] E. Riande, R. Diaz-Calleja, M.G. Prolongo, R.M. Masegosa, C. Salom: Polymer Viscoelasticity, Marcel Dekker, New York (2000).
[23] B.N. Lucas, W.C. Oliver, G.M. Pharr, J.L. Loubet: Mater. Res. Soc. Symp. Proc. 436 (1997) 233.
[24] I.N. Sneddon: Int. J. Eng. Sci. 3 (1965) 47. DOI:10.1016/0020-7225(65)90019-4
[25] J.D. Ferry: Viscoelastic Properties of Polymers, 3rd edition Wiley, New York (1980).
[26] I.M. Low: Mat. Res. Bul. 33 (1998) 1753. DOI:10.1016/S0025-5408(98)00179-2
[27] C.A.Tweedie, K.V. Vliet: J. Mat. Res. 21 (2006) 3029. DOI:10.1557/jmr.2006.0377
[28] G.M. Pharr, A. Bolshakov: J. Mater. Res. 17 (2002) 2660. DOI:10.1557/JMR.2002.0386
[29] F. Bédoui, M. Guigon: Polymer 51 (2010) 5229. DOI:10.1016/j.polymer.2010.08.058

(Received October 29, 2010; accepted December 4, 2011)

Bibliography

DOI 10.3139/146.110687
Int. J. Mat. Res. (formerly Z. Metallkd.)
103 (2012) 6; page 715 – 722

ISSN 1862-5282

Correspondence address

D. Pierre-Emmanuel Mazeran
Laboratoire Roberval, UMR CNRS-UTC 6253,
Université de Technologie de Compiègne
BP 20529, 60205 Compiègne Cedex, France
Tel.: (33) 3 44 23 46 99 (41 29)
Fax: (33) 3 44 23 49 84
E-mail: mazeran@utc.fr

You will find the article and additional material by entering the document number **MK110687** on our website at *www.ijmr.de*